Receptor time integration via discrete sampling

G. Malaguti and P. R. ten Wolde
AMOLF, Science Park 104, 1098 XG Amsterdam, The Netherlands

(Received 15 July 2021; revised 20 October 2021; accepted 11 April 2022; published 11 May 2022)

Living cells can measure chemical concentrations with remarkable accuracy, even though these measurements are inherently noisy due to the stochastic binding of the ligand to the receptor. A widely used mechanism for reducing the sensing error is to increase the effective number of measurements via receptor time integration. This mechanism is implemented via the signaling network downstream of the receptor, yet how it is implemented optimally given constraints on cellular resources such as protein copies and time remains unknown. To address this question, we employ our sampling framework [Govern and ten Wolde, Proc. Natl. Acad. Sci. USA **111**, 17486 (2014)] and extend it here to time-varying ligand concentrations. This framework starts from the observation that the signaling network implements the mechanism of time integration by discretely sampling the ligand-binding state of the receptor and storing these states into chemical modification states of the readout molecules downstream. It reveals that the sensing error has two distinct contributions: a sampling error, which is determined by the number of samples, their independence, and their accuracy, and a dynamical error, which depends on the timescale that these samples are generated. We test our previously identified design principle, which states that in an optimally designed system the number of receptors and their integration time, which determine the number of independent concentration measurements at the receptor level, equals the number of readout proteins, which store these measurements. We show that this principle is robust to the dynamics of the input and the relative costs of the receptor and readout proteins: these resources are fundamental and cannot compensate each other.

DOI: 10.1103/PhysRevE.105.054406

I. INTRODUCTION

It is becoming increasingly clear that living systems can measure chemical concentrations with extraordinary precision. Some animals can smell single molecules [1], swimming bacteria can respond to the binding of a handful of molecules [2,3], and eukaryotic cells can respond to a difference in 10 molecules between the front and the back [4]. An open question is not only what the fundamental limit to the precision of chemical concentration measurements is, but also how cells can reach this limit.

Cells measure chemical concentrations via receptors, which are often located on the cell surface. These measurements are corrupted by noise from the stochastic, diffusive arrival of the ligand molecules at the receptor and from the stochastic binding of the ligand molecules to the receptor proteins, raising the question how cells extract information from the receptor state on the ligand concentration. In recent years different mechanisms have been proposed [5]. One mechanism is that of time integration, first proposed by Berg and Purcell in the context of cellular sensing [2]. In this mechanism cells do not estimate the concentration from the instantaneous ligand binding state of the receptor, but rather from its average over some integration time [2,6–8]. Another mechanism is that of maximum-likelihood sensing [5,9–12], which is based on the idea that the information on the ligand concentration is contained in the receptor time series, and in particular in the duration of the unbound states of the receptor, not the bound states. A related scheme is that of Bayesian filtering [13].

These mechanisms for extracting information from the receptor on the ligand concentration have to be implemented by the signaling network downstream of the receptor. A signaling motif that is very common in both prokaryotes and eukaryotes is the push-pull network. It consists of a cycle of protein activation and deactivation and is often located immediately downstream of the receptor [14] [see Fig. 1(a)]. Examples are GTPase cycles, as in the Ras system, phosphorylation cycles, as in MAPK cascades, and two-component systems like the chemotaxis system of *Escherichia coli*. In the linear regime, the output of these networks depends on a time average of the receptor state. These networks thus allow the cell to implement the mechanism of time integration. In this manuscript, we will study, following our earlier work [15,16], the optimal design of these networks that maximizes the sensing precision given constraints on cellular resources such as protein copies and time.

Ultimately, the cell estimates the ligand concentration from the output of the push-pull network [Fig. 1(a)]. One approach to elucidate the design logic of these systems would be to derive the sensing precision based on this output, for example, by computing the mutual information between the output and the ligand concentration. However, this approach does not naturally elucidate the design logic of this system, because it treats signal transmission from the input L to the output x^* as a black box. The central quantity in this calculation is the covariance σ^2_{L,x^*} between the ligand L and the readout x^*, which does not reveal how the signal is relayed from the input to the output. To elucidate the system's design principles, we

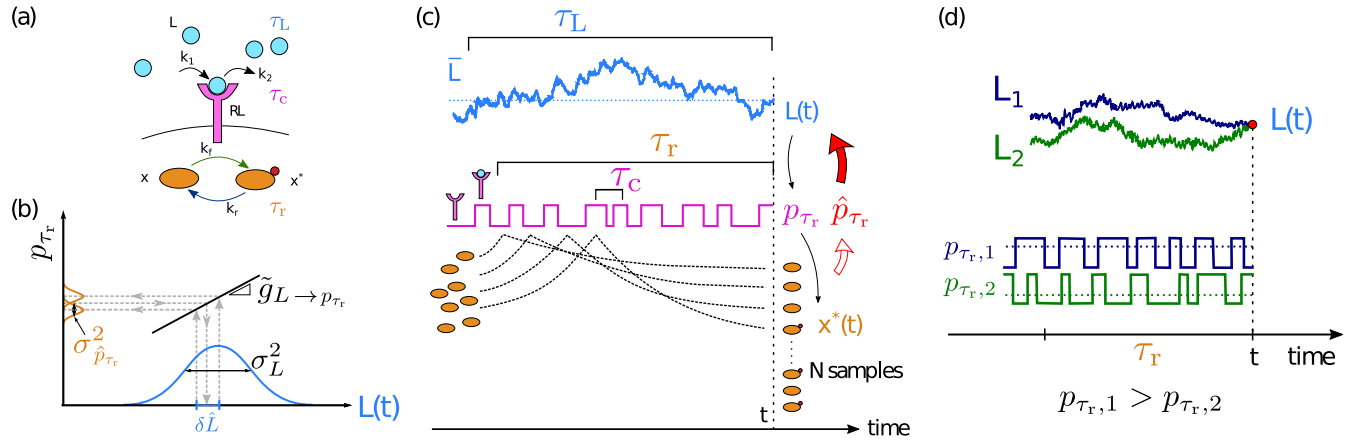

FIG. 1. The precision of estimating a time-varying ligand concentration $L(t)$. (a) The cell signaling network measures the ligand concentration via receptors on its surface. (b) The dynamic input-output relation $p_{\tau_r}(L)$. The cell employs the push-pull network to estimate the average receptor occupancy p_{τ_r} over the past integration time τ_r [see (b)] and then infers the current ligand concentration $L(t)$ by inverting $p_{\tau_r}(L)$. The error in the estimate of the concentration $(\delta\hat{L})^2 = \sigma^2_{\hat{p}_{\tau_r}}/\tilde{g}^2_{L\to p_{\tau_r}}$ depends on the variance $\sigma^2_{\hat{p}_{\tau_r}}$ in the estimate of the average receptor occupancy $\hat{p}_{\tau_r}$ and the dynamic gain $\tilde{g}_{L\to p_{\tau_r}}$, the slope of $p_{\tau_r}(L)$, which determines how the error in $\hat{p}_{\tau_r}$ propagates to that in $\delta\hat{L}$. The input distribution has width σ^2_L. (c) The push-pull network as a sampling device. The network discretely samples the ligand-binding state of the receptor via the readout molecules x [15] and the fraction of modified readout molecules gives the estimate of p_{τ_r}; see Eq. (5). The sensing error has two contributions [Eq. (26)]: the sampling error and the dynamical error. The sampling error arises from the noise in the sampling of the receptor and depends on the number of samples, their independence, and their accuracy. (d) Origin of the dynamical error. The current ligand concentration $L(t)$ is estimated via the average receptor occupancy p_{τ_r} in the past τ_r [see (a)], but the latter depends on the ligand concentration in the past τ_r, which deviates from the current concentration that the cell aims to estimate. Two different input trajectories (L_1 in blue, L_2 in green) ending at time t at the *same* value $L(t)$ (red dot) yield different estimates of $L(t)$ because of their different average receptor occupancies p_{τ_r} over the past τ_r. Figure and caption are adapted from Ref. [16].

have to open the black box: we need to recognize that the input signal is transduced to the output via the receptor, and that the cell does not estimate the ligand concentration from x^* directly, but rather via its receptor [see Fig. 1(a)].

In this paper, we will adopt the sampling framework introduced in Ref. [15], which precisely starts from the observation that the cell uses its push-pull network to estimate the receptor occupancy from which the ligand concentration is then inferred. As we will show, this framework makes it possible to arrive at a much more illuminating form of the same result for the sensing precision. The central idea is that the push-pull network is a discrete sampling device. It implements the mechanism of time integration, not by continuously integrating the state of the receptor, but rather by discretely sampling it, via collisions of the readout molecules with the receptors [Figs. 1(b) and 1(c)]. During each collision, the ligand-binding state of the receptor molecule is copied into the chemical modification state of the readout protein [17]. The readout molecules therefore serve as samples of the receptor molecules, and the fraction of active (modified) readout molecules yields an estimate of the average receptor occupancy. The readout molecules have, however, a finite lifetime, because they can decay or be overwritten via new collisions with the receptor. The estimate of the receptor occupancy is thus an estimate of the average receptor occupancy over this timescale, which is indeed the receptor integration time.

Here we extend the sampling framework of Ref. [15] to time-varying signals and firmly integrate it with our work of Ref. [16]. In Ref. [16] we introduced the concept of the *dynamic* input-output relation for signal transduction via time-varying signals. It gives the mapping between the average receptor occupancy over the past integration time and the current ligand concentration; see Fig. 1(b). The sensing error is then given by the error in the estimate of the receptor occupancy and the slope of the dynamic input-output relation, called the dynamic gain, which determines how the error in the estimate of the receptor occupancy propagates to the error in the estimate of the ligand concentration. In Ref. [16] we derived the dynamic gain, but the error in the estimate of the receptor occupancy was obtained via a route that involved the linear-noise approximation. Here we derive the latter rigorously via the sampling framework of Ref. [15], originally formulated for sensing static concentrations. We show that while in the current paper we focus on push-pull networks in the irreversible limit, the expression for the sensing error has the same form as that for the fully reversible system of Ref. [16]

The benefit of our sampling framework is not only that it provides an illuminating perspective on how cells implement the mathematical operation of time integration via discrete molecules employing a stochastic sampling protocol, but also that it naturally reveals the optimal design that maximizes the sensing precision given constraints on cellular resources, such as protein copies and time. Specifically, this framework predicts that in an optimally designed system the number of receptors and their integration time, which determines the number of independent concentration measurements at the receptor level, equals the number of readout molecules, which store these measurements [15,16]. In Sec. III we will revisit this allocation principle and study how its predictive power depends on the dynamics of the input and the relative costs of the receptor and readout proteins. As we will show, the design

principle is robust, which comes from the fact that these resources are fundamental and cannot compensate each other. In an optimally designed system, each resource is equally limiting, and resources that are in excess can hardly improve the sensing precision.

II. THEORY

A. Model system

Following Ref. [16], we analyze a living cell that measures a ligand concentration that varies in time. The concentration is detected via receptors that drive a push-pull network; see Fig. 1(a). The model is identical to that of Ref. [16], except that the push-pull network operates in the irreversible limit. This is a reasonable assumption for living systems, since these push-pull networks are typically driven out of thermodynamic equilibrium via the turnover of ATP and inside the living cell the free energy of ATP hydrolysis is about $20k_BT$. While the model is indeed very similar to that of Ref. [16], we briefly summarize its main elements, which are necessary to understand our theory and the results.

We model the ligand concentration as a stationary Markovian signal, obeying Gaussian statistics [18]. The signal is characterized by the mean (total) ligand concentration $\overline{L}$, the variance σ_L^2, and the correlation time τ_L.

We imagine that the receptor proteins R bind the ligand molecules L independently [5], $L + R \underset{k_2}{\overset{k_1}{\rightleftharpoons}} RL$. The correlation time of the ligand-binding state of the receptor is given by $\tau_c = 1/(k_1\overline{L} + k_2)$, and it sets the timescale on which independent concentration measurements can be taken. Denoting the total receptor copy number by R_T and the average number of ligand-bound receptors as $\overline{RL}$, the receptor occupancy is $p = \overline{RL}/R_T = k_1\overline{L}\tau_c$. Hence, for a given occupancy p the correlation time $\tau_c = p/(k_1\overline{L})$ is constrained by the average ligand concentration $\overline{L}$ and its diffusion constant, which limits the binding rate k_1 [2,5–7].

The push-pull network measures the ligand-binding state of the receptor [14]. In this network, fuel turnover is used to drive the chemical modification of a downstream readout protein x, for example, phosphorylation via the hydrolysis of adenosine triphosphate (ATP). The receptor, or its associated enzyme like CheA in the *E. coli* chemotaxis system, catalyses the modification of the readout, $x + \mathrm{RL} + \mathrm{ATP} \rightleftharpoons x^* + \mathrm{RL} + \mathrm{ADP}$. The active readout x^* decays naturally or via an enzyme, like CheZ in the *E. coli* chemotaxis system, $x^* \rightleftharpoons x + \mathrm{Pi}$. The cellular metabolism keeps the signaling network out of thermodynamic equilibrium by fixing the concentrations of ATP, ADP (adenosine diphosphate), and Pi (inorganic phosphate). In this manuscript we will exploit that inside the living the cell the concentrations of ATP, ADP, and Pi are kept so far out of thermodynamic equilibrium that the microscopic reverse reactions of receptor/kinase catalyzed phosphorylation, i.e., the dephosphorylation reaction $x^* + \mathrm{RL} + \mathrm{ADP} \to x + \mathrm{RL} + \mathrm{ATP}$ and (phosphatase-catalyzed) dephosphorylation, i.e., the phosphorylation reaction $x + \mathrm{Pi} \to x^*$, do not happen. The concentrations of ATP, ADP, and Pi and the activities of the enzymes are absorbed in the (de)phosphorylation rates, coarse graining the (de)modification reactions into instantaneous second-order reactions. The network is therefore described by $x + \mathrm{RL} \xrightarrow{k_f} x^* + \mathrm{RL}$, $x^* \xrightarrow{k_r} x$. The relaxation time of this network is $\tau_r = 1/(k_f\overline{\mathrm{RL}} + k_r)$, and it is the timescale on which the readout correlation function decays when the ligand concentration is constant [15]. This relaxation time determines the lifetime of the active readout molecules, and hence the timescale on which the readout can carry information on the ligand binding state of the receptor in the past. The relaxation time τ_r is indeed the receptor integration time.

B. The cell sensing precision

1. Overview and relation to earlier work

The derivation of the central result, Eq. (26), is based on the dynamic input-output relation; see Fig. 1(b). Below we first describe that relation. We then show that the sensing error is given by two factors: (1) the slope of this input-output relation, called the dynamic gain, and (2) the error in estimating the receptor occupancy; see Eq. (1). The concept of the dynamic input-output relation was first introduced in Ref. [16] and the dynamic gain was first derived in Ref. [16]. To keep the paper self-contained, we will briefly describe these elements of our theory, but for their mathematical derivation we refer to Ref. [16]. The second factor, the error in estimating the receptor occupancy, was also derived in Ref. [16], yet via a route based on the linear-noise approximation. Here we show that it can be rigorously derived via the sampling framework first introduced in Ref. [15] in the context of sensing static signals; indeed, the novelty in the derivation of the central result, Eq. (26), is the extension of the sampling framework to time-varying signals.

2. Dynamic input-output relation

As first proposed in Ref. [16], the cell uses the signaling network to estimate the average occupancy p_{τ_r} of the receptor over the past integration time τ_r, and then uses this estimate $\hat{p}_{\tau_r}$ to obtain an estimate for the current concentration L by inverting the mapping $p_{\tau_r}(L)$. The function $p_{\tau_r}(L)$ is the *dynamic input-output relation*, and it gives the mapping between the average receptor occupancy p_{τ_r} over the *past* integration time τ_r and the *current* value of the input signal $L = L(t)$; see Fig. 1(b). The average is taken not only over the fluctuations in receptor-ligand binding and readout (de)activation [Fig. 1(c)], but also over the ensemble of ligand trajectories in the past that all end at the same current ligand concentration L [Fig. 1(d)] [18–20]. The dynamic input-output relation reduces to the static input-output relation when the input timescale τ_L is much longer than the receptor correlation time τ_c and integration time τ_r.

3. Sensing error

Linearizing the dynamic input-output relation $p_{\tau_r}(L)$ around the mean ligand concentration $\overline{L}$ [see Fig. 1(b)] and employing the rules of error propagation yields, as shown in Ref. [16], the expected error in the concentration estimate:

$$(\delta\hat{L})^2 = \frac{\sigma^2_{\hat{p}_{\tau_r}}}{\tilde{g}^2_{L\to p_{\tau_r}}}. \tag{1}$$

The quantity $\tilde{g}_{L\to p_{\tau_r}}$ is the *dynamic* gain. It is the slope of the dynamic input-output relation $p_{\tau_r}(L)$ and describes how an error in the estimate of p_{τ_r} translates to an error in the estimate of L. The quantity $\sigma^2_{\hat{p}_{\tau_r}}$ is the variance in the estimate $\hat{p}_{\tau_r}$ of the average receptor occupancy over the past τ_r given that the current input signal is L; see Fig. 1(b).

The signal-to-noise ratio (SNR) is then given by

$$\mathrm{SNR} \equiv \frac{\sigma_L^2}{(\delta\hat{L})^2} = \frac{\tilde{g}^2_{L\to p_{\tau_r}}}{\sigma^2_{\hat{p}_{\tau_r}}}\,\sigma_L^2. \tag{2}$$

Here σ_L^2 is the variance of the ligand concentration L; it is a measure for the total number of input states. The signal-to-noise ratio thus quantifies the number of distinct ligand concentrations that the system can resolve. The signal-to-noise ratio also yields the mutual information $I(L;x^*) = 1/2\ln[1+\mathrm{SNR})]$ between the input L and output x^* [18].

4. Dynamic gain

As derived in Ref. [16], the dynamic gain is given by

$$\tilde{g}_{L\to p_{\tau_r}} = \frac{p(1-p)}{\overline{L}}\left(1+\frac{\tau_c}{\tau_L}\right)^{-1}\left(1+\frac{\tau_r}{\tau_L}\right)^{-1} \tag{3}$$

$$= g_{L\to p}\left(1+\frac{\tau_c}{\tau_L}\right)^{-1}\left(1+\frac{\tau_r}{\tau_L}\right)^{-1}. \tag{4}$$

The dynamic gain depends on the timescales of both the input signal and the system. Only when $\tau_L \gg \tau_r, \tau_c$ is the average ligand concentration over the subensemble of trajectories ending at $\delta L(t)$ equal to the current concentration $\delta L(t)$ [see Fig. 1(d)], and does $\tilde{g}_{L\to p_{\tau_r}}$ become equal to its maximal value, the static gain $g_{L\to p} = p(1-p)/\overline{L}$.

5. The error in estimating the receptor occupancy

To arrive at an illuminating expression for the error in the estimate of p_{τ_r}, $\sigma^2_{\hat{p}_{\tau_r}}$, we adopt the perspective of Ref. [15], which views the push-pull network as a sampling device, taking samples of the receptor state in a discrete fashion [see Fig. 1(c)]. Below we first briefly describe the principal ideas of the sampling framework [15]. This not only serves to keep our paper self-contained, but also to introduce the new elements in extending this framework to time-varying signals.

The sampling framework. Samples are created via the activation reaction $x + \mathrm{RL} \to x^* + \mathrm{RL}$, which copies the ligand-binding state of the receptor in stable modification states of the readout molecules [Fig. 1(c)]. The readout molecules thus constitute samples of the receptor molecules, and together they encode the occupancy of the receptor in the past. The effective number of independent samples depends not only on the creation of samples, but also on their decay and accuracy. The deactivation reaction $x^* \to x$ erases samples, which means that the samples only contain information on the receptor state over the past τ_r. In addition, both the activation and the deactivation reaction could in principle happen in their microscopic reverse direction, which would reduce the accuracy of the samples by corrupting the coding. However, since push-pull networks are typically driven far out of equilibrium, we will ignore this here. All of the receptor samples x^* will thus be fully accurate. Furthermore, for signals that vary in time, we also need to recognize that the samples correspond to the ligand concentration over the past integration time τ_r, and not the current concentration, which is the concentration that the cell aims to estimate. A finite τ_r is necessary for reducing the receptor sampling noise via time integration, but, as we will see, it will also yield a systematic error in the concentration estimate that the cell cannot reduce by taking more receptor samples.

Specifically, recognizing that the current number of active readout molecules $x^*(L(t)) = x^*(L)$ equals the number of samples of receptors that are bound to ligand in the past integration time τ_r, it becomes clear that the cell estimates the average receptor occupancy p_{τ_r} over the past τ_r from the fraction [15]:

$$\hat{p}_{\tau_r} = \frac{x^*(L)}{\overline{N}}, \tag{5}$$

where $\overline{N}$ is the average total number of samples obtained during τ_r, corresponding to both ligand-bound and ligand-unbound receptors. The number of active readout molecule $x^*(t)$ at time t is given by

$$x^*(t) = \sum_{i=1}^{N} n_i(t_i), \tag{6}$$

where n_i is the state of the ith sample, corresponding to the state of the receptor involved in the ith collision at time $t_i < t$: $n_i(t_i) = 1$ if the receptor is ligand bound and $n_i(t_i) = 0$ otherwise. The total rate at which inactive readout molecules interact with the receptor—the sampling rate—is given by $r = k_f \bar{x} R_T$ and the average number of samples obtained during the integration time τ_r is

$$\overline{N} = k_f \bar{x} R_T \tau_r. \tag{7}$$

We also note here that the flux of readout molecules is $\dot{n} = rp$. Moreover, noting that $f = k_f p R_T \tau_r$, the sampling rate is also given by $r = f(1-f)X_T/(p\tau_r)$ while the average number of samples obtained during the integration time can be written as $\overline{N} = f(1-f)X_T/p$. As we will show below, the variance in the estimate of p_{τ_r} in Eq. (5), $\sigma^2_{\hat{p}_{\tau_r}}$ [Eq. (1)], can be understood in terms of the error of a sampling protocol: it depends on the number of samples, their independence (their accuracy, although that is not derived here, but see [16]), and the timescale on which they are generated.

Decomposing the sampling error. Figure 2 gives an overview of our scheme to compute the variance in the estimate of the receptor occupancy, $\sigma^2_{\hat{p}_{\tau_r}}$. Using the law of total variance, the error $\sigma^2_{\hat{p}_{\tau_r}}$ in the estimate of the receptor occupancy p_{τ_r} over the past integration time τ_r is given by

$$\sigma^2_{\hat{p}_{\tau_r}} = \mathrm{var}\big[E\left(\hat{p}_{\tau_r}|N\right)\big] + E\big[\mathrm{var}\left(\hat{p}_{\tau_r}|N\right)\big]. \tag{8}$$

The first term reflects the variance of the mean of $\hat{p}_{\tau_r}$ given the number of samples N; the second term reflects the mean of the variance in $\hat{p}_{\tau_r}$ given the number of samples N [15]. As we show next, these terms can be decomposed and recombined such that the error in estimating p_{τ_r} can be written as

$$\sigma^2_{\hat{p}_{\tau_r}} = \sigma^{2,\mathrm{samp}}_{\hat{p}_{\tau_r}} + \sigma^{2,\mathrm{dyn}}_{\hat{p}_{\tau_r}}. \tag{9}$$

Error from stochasticity in number of samples. The first term of Eq. (8) describes the noise that arises from the

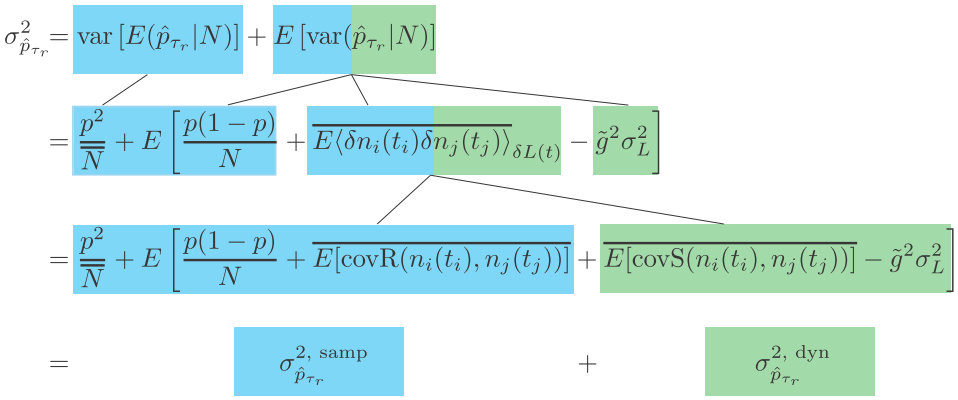

FIG. 2. Overview of the decomposition of the variance $\sigma^2_{\hat{p}_{\tau_r}}$ in the estimate $\hat{p}_{\tau_r}$ of the receptor occupancy p_{τ_r} over the past integration τ_r given that the current ligand concentration $L(t) = L$. The error in the estimate of p_{τ_r} can be decomposed into the sampling error $\sigma^{2,\mathrm{samp}}_{\hat{p}_{\tau_r}}$, denoted in blue, and the dynamical error $\sigma^{2,\mathrm{dyn}}_{\hat{p}_{\tau_r}}$, denoted in green [see Eq. (9)]. The sampling error is a statistical error, arising from the finite cellular resources to sample the state of the receptor; see Eq. (22). The dynamical error is a systematic error that arises from the input dynamics and depends only on timescales; see Eq. (24). To arrive at this decomposition, $\sigma^2_{\hat{p}_{\tau_r}}$ is split into a contribution from the stochasticity in the number of samples ("variance of the mean") and one from the error for a fixed number of samples ("mean of the variance"); see Eq. (8). The first is given by Eq. (10). The latter consists of three contributions and is given by Eq. (12). The second of these three, the receptor covariance, contributes both to the sampling error [see Eq. (17)] and the dynamical error [see Eq. (23)].

stochasticity in the number of samples. It can be written as (see Appendix A)

$$\mathrm{var}\big[E\left(\hat{p}_{\tau_r}|N\right)\big] = \frac{p^2}{\overline{N}}. \tag{10}$$

This contribution reflects the fact that with a push-pull network as considered here, the cell cannot discriminate between those readout molecules that have collided with an unbound receptor, and hence provide a sample of the receptor, and those that have not collided with a receptor at all; this term is zero for a bifunctional kinase where the unbound receptor catalyzes readout deactivation [15]. This term contributes to $\sigma^{2,\,\mathrm{samp}}_{\hat{p}_{\tau_r}}$ in Eq. (9).

Error for fixed number of samples. The second term of Eq. (8) describes the error in the estimate of p_{τ_r} that arises for a fixed number of samples. It is given by

$$E[\mathrm{var}(\hat{p}_{\tau_r}|N)] = E\left[\frac{N^2}{\overline{N^2}}\mathrm{var}\left(\frac{\sum_{i=1}^N n_i(t_i)}{N}\middle|N\right)\right]. \tag{11}$$

In Appendix B we show that

$$\mathrm{var}\left(\frac{\sum_{i=1}^N n_i(t_i)}{N}\middle|N\right) = \frac{p(1-p)}{N} + \overline{E\langle\delta n_i(t_i)\delta n_j(t_j)\rangle}_{\delta L(t)} - \tilde{g}^2\sigma_L^2, \tag{12}$$

where $\delta n_i(t_i) = n_i(t_i) - p$, E denotes an average over the sampling times t_i, and the overline an average over δL. As we show next, the receptor covariance $\overline{E\langle\delta n_i(t_i)\delta n_j(t_j)\rangle}_{\delta L(t)}$ splits into two contributions, one that together with the first term of Eq. (12) and with Eq. (10) forms the sampling error, and one that together with the last term of Eq. (12), $-\tilde{g}^2\sigma_L^2$, forms the dynamical error of Eq. (23); see Fig. 2.

The receptor covariance. To derive the receptor covariance $\overline{E\langle\delta n_i(t_i)\delta n_j(t_j)\rangle}_{\delta L(t)}$, the second term of Eq. (12), we note that the deviation $\delta n_i(t_i) = n_i(t_i) - p$ of the receptor occupancy $n_i(t_i)$ from the mean p is

$$\delta n_i(t_i) = \int_{-\infty}^{t_i} dt' e^{-(t_i-t')/\tau_c}[\rho_n\,\delta L(t') + \xi_i(t')], \tag{13}$$

where $\xi_i(t')$ models the ligand-binding noise of the receptor i at time t'. The covariance for a given $\delta L(t)$ is then given by the sum of two contributions,

$$\langle\delta n_i(t_i)\delta n_j(t_j)\rangle_{\delta L(t)} = \underbrace{\rho_n^2\int_{-\infty}^{t_i} dt'\int_{-\infty}^{t_j} dt'' e^{-(t_i-t')/\tau_c}\langle\delta L(t')\delta L(t'')\rangle_{\delta L(t)} e^{-(t_j-t'')/\tau_c}}_{\mathrm{covS}} + \underbrace{\int_{-\infty}^{t_i} dt'\int_{-\infty}^{t_j} dt'' e^{-(t_i-t')/\tau_c}\langle\xi_i(t')\xi_j(t'')\rangle e^{-(t_j-t'')/\tau_c}}_{\mathrm{covR}}. \tag{14}$$

Hence, the receptor covariance averaged over $\delta L(t)$ and the sampling times is

$$\overline{E\langle\delta n_i(t_i)\delta n_j(t_j)\rangle}_{\delta L(t)} = \overline{E[\mathrm{covS}(n_i(t_i), n_j(t_j))]} + \overline{E[\mathrm{covR}(n_i(t_i), n_j(t_j))]}. \tag{15}$$

The first term on the right-hand side of Eq. (15) describes the receptor covariance due to the ligand concentration dynamics. Together with the third term of Eq. (12), $-\tilde{g}^2\sigma_L^2$, it forms the dynamical error in estimating p_{τ_r}; see Fig. 2. The second term of Eq. (15) characterizes the correlations in the receptor switching that arise from the stochastic ligand binding and unbinding. This term forms, together with Eq. (10) and with the first term of Eq. (12), the sampling error in estimating p_{τ_r}; see Fig. 2. We will now first show how these three terms yield the sampling error. We will then return to the first term on the right-hand side of Eq. (15) and show how that with $-\tilde{g}^2\sigma_L^2$ it forms the dynamical error.

Receptor switching noise. In Eq. (14), $\langle \xi_i(t')\xi_j(t'')\rangle = \langle \xi^2\rangle \delta_{ij}\delta(t'-t'')$ where the noise amplitude $\langle \xi^2\rangle = 2p(1-p)/\tau_c$ and the Kronecker delta δ_{ij} captures our assumption that the ligand molecules bind the receptors independently, thus ignoring spatiotemporal correlations [5]. The second term of Eq. (14) then yields

$$\mathrm{covR}(n_i(t_i), n_j(t_j)) = p(1-p)\delta_{ij}e^{-|t_j-t_i|/\tau_c}. \tag{16}$$

We now perform the averaging over the sampling times, denoted by E. In Appendix C we show that this yields

$$E[\mathrm{covR}(n_i(t_i), n_j(t_j))] = \frac{p(1-p)}{R_T}\frac{\tau_c}{\tau_r}. \tag{17}$$

The above expression is the same for each signal value $\delta L(t)$ and hence also equals $\overline{E[\mathrm{covR}(n_i(t_i), n_j(t_j))]}$.

The sampling error. Equation (17) forms with the first term of Eq. (12) the sampling error for a fixed number of samples N (see Ref. [15]):

$$\mathrm{var}\left(\frac{\sum_{i=1}^N n_i(t_i)}{N}\right)^{\mathrm{samp}} = \frac{p(1-p)}{N}\left(1+\frac{2N\tau_c}{2R_T\tau_r}\right) \tag{18}$$

$$= \frac{p(1-p)}{f_I N}, \tag{19}$$

where

$$f_I = \frac{1}{1+2\tau_c/\Delta} \tag{20}$$

is the fraction of independent samples with $\Delta = 2R_T\tau_r/N$ being the spacing between the receptor samples. Clearly, if the sampling interval Δ is much larger than the receptor correlation time τ_c, all samples are independent and $f_I \to 1$.

We now have to average Eq. (19) over the different number of samples N [see Eq. (11)], which finally gives

$$E[\mathrm{var}(\hat{p}_{\tau_r}|N)]^{\mathrm{samp}} = \frac{p(1-p)}{f_I\overline{N}} = \frac{p(1-p)}{\overline{N}_I}. \tag{21}$$

This equation has a very clear interpretation: it is the error in the estimate of the receptor occupancy based on a single measurement—given by the variance of the receptor occupancy $p(1-p)$—divided by the total number of independent measurements $\overline{N}_I \equiv f_I\overline{N}$.

Equations (10) and (21) together yield the sampling error in estimating the receptor occupancy

$$\sigma^{2,\mathrm{samp}}_{\hat{p}_{\tau_r}} = \frac{p^2}{\overline{N}} + \frac{p(1-p)}{f_I\overline{N}}. \tag{22}$$

Both contributions to $\sigma^{2,\mathrm{samp}}_{\hat{p}_{\tau_r}}$ are governed by the nature of the receptor sampling process and do not depend on the input statistics. They are indeed the same as those for sensing static concentrations, derived previously [15].

Dynamical error. In estimating a time-varying ligand concentration, the sensing error arises not only from the stochastic sampling of the receptor state, but also from the fact that the current ligand concentration corresponds to an ensemble of ligand trajectories in the past, which each give rise to a different integrated receptor occupancy. This effect is contained in the first term of Eq. (15). In Appendix D we show that

$$\overline{E[\mathrm{covS}(n_i(t_i), n_j(t_j))]} = \tilde{g}^2\sigma_L^2\left(1+\frac{\tau_c}{\tau_L}\right)\left(1+\frac{\tau_r}{\tau_L}\right)\left(1+\frac{\tau_c\tau_r}{\tau_L(\tau_c+\tau_r)}\right). \tag{23}$$

Importantly, the above expression is not the dynamical error in the estimate of the receptor occupancy. It is the receptor covariance that arises from the signal dynamics, but this contains a contribution from the dynamical error [i.e., the variance in p_{τ_r} due to different past ligand trajectories ending at the same $L(t)$; see Fig. 2(c)] *and* the signal variations of interest, $\tilde{g}^2\sigma_L^2$ [i.e., the variance in p_{τ_r} resulting from variations in $L(t)$]. To obtain the dynamical error in the receptor occupancy, we have to subtract from the above expression $\tilde{g}^2\sigma_L^2$, which is indeed the third term of Eq. (12)—the term that we had not yet taken care of (see also Fig. 2). This procedures directly yields the dynamical error in the receptor occupancy, because the above expression does not depend on the number of samples N, so there is no need to average over N in Eq. (11). We thus immediately find

$$\sigma^{2,\ \mathrm{dyn}}_{\hat{p}_{\tau_r}} = \tilde{g}^2\sigma_L^2\left[\left(1+\frac{\tau_c}{\tau_L}\right)\left(1+\frac{\tau_r}{\tau_L}\right)\left(1+\frac{\tau_c\tau_r}{\tau_L(\tau_c+\tau_r)}\right)-1\right]. \tag{24}$$

This error corresponds indeed to the variation in p_{τ_r} that arises from the different concentration trajectories in the past τ_r that each end at $\delta L(t)$; see Fig. 1(d). It does depend on the statistics of the input signal: it increases with the width of the input distribution, σ_L^2, and decreases with the input timescale τ_L.

Together, the sampling error [Eq. (22)] and the dynamical error [Eq. (24)] determine the total error in estimating the receptor occupancy [Eq. (9)]:

$$\sigma^2_{\hat{p}_{\tau_r}} = \frac{p^2}{\overline{N}} + \frac{p(1-p)}{f_I\overline{N}} + \tilde{g}^2\sigma_L^2\left[\left(1+\frac{\tau_c}{\tau_L}\right)\times\left(1+\frac{\tau_r}{\tau_L}\right)\left(1+\frac{\tau_c\tau_r}{\tau_L(\tau_c+\tau_r)}\right)-1\right]. \tag{25}$$

6. Central result

Equation (25) gives the error in the estimate of the average receptor occupancy p_{τ_r}, and to understand how this error propagates to the error $(\delta\hat{L})^2$ in the estimate of the ligand concentration, we divide $\sigma^2_{\hat{p}_{\tau_r}}$ by the dynamic gain $\tilde{g}_{L\to p_{\tau_r}}$

given by Eq. (3) [see Eq. (2)]:

$$\mathrm{SNR}^{-1} = \underbrace{\left(1+\frac{\tau_c}{\tau_L}\right)^2\left(1+\frac{\tau_r}{\tau_L}\right)^2\left[\frac{\left(\overline{L}/\sigma_L\right)^2}{p(1-p)\overline{N}_I}+\frac{\left(\overline{L}/\sigma_L\right)^2}{(1-p)^2\overline{N}_{\mathrm{eff}}}\right]}_{\text{sampling error}} + \underbrace{\left(1+\frac{\tau_c}{\tau_L}\right)\left(1+\frac{\tau_r}{\tau_L}\right)\left(1+\frac{\tau_c\tau_r}{\tau_L(\tau_c+\tau_r)}\right)-1}_{\text{dynamical error}}. \quad (26)$$

This expression gives the signal-to-noise ratio for the irreversible push-pull network in terms of the total number of receptor samples, their independence, and the timescale on which they are generated. The expression is the same as that obtained from a straightforward calculation based on the linear-noise approximation (see Appendix E), but it is much more illuminating. It shows that the sensing error SNR^{-1} can be decomposed into two distinct contributions. One is the *sampling error*, which arises from the stochasticity in the sampling of the receptor state, i.e., the first two terms on the right-hand side of Eq. (25). The other is the *dynamical error* and originates from the dynamics of the input signal, i.e., the last term of Eq. (25).

Interestingly, this result is identical to that of the fully reversible system, derived in Ref. [16]. The only difference is in the expressions for $\overline{N}_{\mathrm{eff}}$, which is the total number of effective samples, and $\overline{N}_{\mathrm{I}}$, which is the number of these that are independent [15,16]. For the fully *reversible* system they are given by

$$\overline{N}_{\mathrm{I}} = \underbrace{\frac{1}{1+2\tau_c/\Delta}}_{f_I}\underbrace{\overbrace{\frac{(e^{\beta\Delta\mu_1}-1)(e^{\beta\Delta\mu_2}-1)}{e^{\beta\Delta\mu}-1}}^{q}\overbrace{\frac{\dot{n}\tau_r}{p}}^{\bar{N}}}_{\bar{N}_{\mathrm{eff}}}. \quad (27)$$

The quantity $\dot{n}$ is the net flux of x around the cycle of activation and deactivation, which for the fully reversible system is given by $\dot{n} = k_{\mathrm{f}}pR_{\mathrm{T}}\bar{x} - k_{-\mathrm{f}}pR_{\mathrm{T}}\bar{x}^*$, yet for the irreversible system reduces to $\dot{n} = k_{\mathrm{f}}pR_{\mathrm{T}}\bar{x}$. The quantity $\dot{n}/p$ is thus the sampling rate r of the receptor, be it ligand bound or not. The principal difference between the result for the reversible system of Ref. [16] and that for the irreversible system studied here concerns the accuracy of sampling, which is quantified by the quality factor q, where $\Delta\mu = \Delta\mu_1 + \Delta\mu_2$ and $\Delta\mu_1$ and $\Delta\mu_2$ quantify, respectively, how much the modification and demodification reactions are driven out of thermodynamic equilibrium. For the irreversible system $\Delta\mu_1, \Delta\mu_2 \to \infty$, and the quality factor q reaches unity: when a receptor sample is taken, the ligand-binding state of a receptor protein is accurately copied into the modification state of a readout molecule. For the irreversible system studied here, all samples are thus effective, such that the average number of effective samples $\overline{N}_{\mathrm{eff}}$ equals the average number of total samples $\overline{N}$, $\overline{N}_{\mathrm{eff}} = \overline{N}$. The factor f_I describes for both the reversible and the irreversible system as discussed above [see also Eq. (20)], the fraction of samples that are independent, with $\Delta = 2\tau_r/(\overline{N}_{\mathrm{eff}}/R_{\mathrm{T}})$ the average receptor sampling interval. For the irreversible system studied here, the average number of independent samples is indeed $\overline{N}_{\mathrm{I}} = f_I\overline{N}$ [see also Eq. (21)].

While the first term inside the square brackets of Eq. (26) describes how the sampling error depends on the number of samples, their independence, and their accuracy, the second term describes how the sampling error depends on their distinguishability. This term stems from Eq. (10), which quantifies the error that arises from the fact that with the push-pull network considered here the cell cannot discriminate between readout molecules that have interacted with an unbound receptor and those that have not interacted with a receptor at all. This term is indeed zero for a readout system based on a bifunctional kinase, where phosphorylated readout proteins do not decay spontaneously but only via reactions catalyzed by unbound receptors—such that, in the irreversible limit studied here, a phosphorylated readout molecule always constitutes a sample of a bound receptor and an unphosphorylated readout molecule always forms a sample of an unbound receptor. This distinguishability enhances the sensing precision.

The second distinct contribution to the sensing error, the dynamical error [16], depends only on timescales and not on the accuracy of sampling. Indeed, when the number of samples becomes infinite and the sampling error goes to zero, the sensing error remains nonzero because of the dynamical error. The latter is a systematic (as opposed to random) error in estimating L, which only reduces to zero when the receptor correlation time τ_c and the integration time τ_r are much smaller than the timescale τ_L on which the ligand fluctuates.

Equation (26) also highlights that the integration time τ_r affects the sensing precision via three distinct mechanisms. Increasing the integration time increases the number of samples $\overline{N}$—this is indeed the mechanism of time integration. Yet increasing τ_r also increases the dynamical error and reduces the dynamic $\tilde{g}_{L\to p_{\tau_r}}$, corresponding to the prefactor of the sampling error in front of the square brackets. As we will see, the interplay between these three factors gives rise to an optimal integration time that maximizes the sensing precision.

In summary, the principal result of Ref. [16], Eq. (26), can, at least for the irreversible system studied here, be rigorously derived from the idea that the push-pull network is a system that samples the state of the receptor by copying its ligand-binding state into chemical modification states of readout proteins. It elucidates how the sensing precision depends on the number of samples, their accuracy, their independence, their distinguishability, and the timescale on which they are taken compared to that of the input signal.

III. RESULTS

A. Optimal allocation principle revisited

Figure 3(a) shows the sensing precision as quantified by the mutual information $I(x^*;L)$ between the number of active readout proteins x^* and the ligand concentration L as a function of the number of receptors R_{T} and the total number

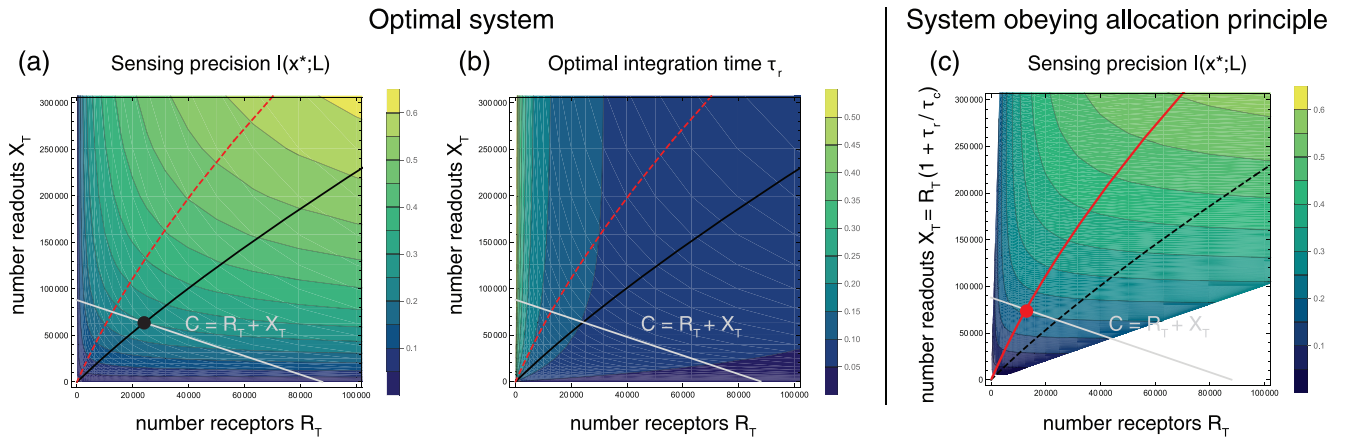

FIG. 3. Design of the optimal sensing system. (a) Sensing precision of the optimal system, as quantified via the mutual information $I(x^*;L)$, as a function of the number of receptors R_T and the number of readout proteins X_T, where $I(x^*;L)$ has been optimized over the integration time τ_r and the receptor occupancy p. The gray line shows one contour line of a constant total protein cost $C = R_T + X_T$. The black point on this line is the combination of the number of receptors R_T and readout proteins X_T that maximizes the sensing precision $I(x^*;L)$ along this contour line of constant protein cost C. The black line shows the optimal design (R_T, X_T) that maximizes the sensing precision $(I(x^*;L)$ for a given protein cost C, as a function of C. The red dashed line is the same parametric plot but then for a system that is constrained to obey the optimal allocation principle $X_T = R_T(1 + \tau_r/\tau_c)$. (b) The optimal integration time that maximizes the mutual information as shown in (a) as a function of the number of receptors R_T and readout proteins X_T. (c) Sensing precision $I(x^*;L)$ as a function of R_T and X_T for a system that obeys the resource allocation principle $X_T = R_T(1 + \tau_r/\tau_c)$, where $I(x^*;L)$ has been optimized over the receptor occupancy p (and the integration time τ_r is set by the allocation principle). The red point shows the combination of R_T and X_T that maximizes $I(x^*;L)$ along the shown contour line of constant protein cost $C = R_T + X_T$. The red line shows the parametric plot of (R_T, X_T) that maximizes $I(x^*;L)$ for a given C, as a function of C. For ease of comparison, this line is shown as a red dashed line in (a); similarly, the black solid line of panel (a), showing the optimal design (R_T, X_T) as a function of protein cost C, is shown here as black dashed line. Since the minimal integration time τ_r is zero, no system obeying the allocation principle $X_T = R_T(1 + \tau_r/\tau_c)$ exists for which $X_T < R_T$. The receptor correlation time is $\tau_c/\tau_L = 10^{-2}$, and the relative width of the signal distribution is $\sigma_L/\bar{L} = 10^{-2}$.

of readout proteins X_T. Here we have optimized, for each R_T and X_T, over the receptor occupancy p and the integration time τ_r, while keeping the receptor correlation time τ_c and the input statistics given by σ_L and τ_L constant. It is seen that the sensing precision increases when R_T and X_T are increased together. In contrast, when either X_T or R_T is increased while keeping the other component constant, the mutual information will first rise but then saturate, as described in Refs. [15,16]. This shows that both resources are fundamental, and cannot compensate each other in reaching a desired sensing precision [15,16].

Figure 3(b) shows the optimal integration time $\tau_r^{\rm opt}$ that maximizes the sensing precision as a function of R_T and X_T. It is seen that for a given R_T, $\tau_r^{\rm opt}$ first rises with X_T but then reaches a plateau. Conversely, the optimal integration time $\tau_r^{\rm opt}$ decreases to zero when R_T is increased at fixed X_T.

These observations can be understood using the optimal resource allocation principle uncovered in Refs. [15,16]. This principle is derived from the identification of the fundamental resources for sensing. As explained in in Refs. [15,16], a fundamental resource is a collective variable Q_i that, when set to a constant value, puts a nonzero lower bound on SNR^{-1}, irrespective of how the other variables are changed. Mathematically, it is defined as $\mathrm{MIN}_{Q_i=\mathrm{const}}(\mathrm{SNR}^{-1}) = f(\mathrm{const}) > 0$. These collective variables can be identified by numerically or analytically minimizing SNR^{-1}, constraining (combinations of) variables yet optimizing over the other variables. Applying this procedure reveals that the sensing precision of the irreversible system studied here is bounded:

$$\mathrm{SNR}^{-1} \geqslant \left(1 + \frac{\tau_r}{\tau_L}\right)^2 \frac{4(\bar{L}/\sigma_L)^2}{R_T(1 + \tau_r/\tau_c)} + \frac{\tau_r}{\tau_L} \tag{28}$$

$$\geqslant \left(1 + \frac{\tau_r}{\tau_L}\right)^2 \frac{4(\bar{L}/\sigma_L)^2}{X_T} + \frac{\tau_r}{\tau_L}. \tag{29}$$

The first bound corresponds to the limit in which R_T is limiting and X_T is abundant, while the second bound corresponds to the opposite regime. Crucially, these bounds differ only in the expressions in the denominator in the first term. This indicates that in an optimally designed system the following resource allocation principle is obeyed [15,16]:

$$R_T(1 + \tau_r/\tau_c) \approx R_T\tau_r/\tau_c \approx X_T, \tag{30}$$

where we have exploited that the receptor integration time τ_r is typically larger than the receptor correlation time τ_c, which is indeed a prerequisite for time integration; for the *E. coli* chemotaxis system, τ_r/τ_c is about 5–50 [16]. The prediction of Eq. (30) has a clear interpretation: $R_T\tau_r/\tau_c$ is the number τ_r/τ_c of independent concentration measurements per receptor times the total number of receptors R_T. This product $R_T\tau_r/\tau_c$ equals the total number of independent concentration measurements at the receptor level, since we have assumed here that the receptors measure the concentration independently (for the effect of receptor correlations, see [5]). In an optimally designed system, the number of independent measurements at the receptor level, $R_T\tau_r/\tau_c$ also equals the number of readout proteins X_T that are needed to store these measurements.

The design principle Eq. (30) can perhaps be best understood by focusing on the receptor sampling interval Δ. For any system, the sampling interval is $\Delta = 2R_T\tau_r/\overline{N}$ while the average number of samples equals $\overline{N} = f(1-f)X_T/p$, as discussed above. Moreover, an inspection of Eq. (26) reveals that in the optimal system that maximizes the sensing precision, the active readout fraction $f \to 1/2$, while the allocation principle Eq. (30) predicts that $X_T \approx R_T\tau_r/\tau_c$, such that the sampling interval of the optimal system is predicted to be

$$\Delta^{\text{opt}} \approx 8\tau_c p^{\text{opt}}. \tag{31}$$

A numerical optimization of Eq. (26) over p, imposing the allocation principle $X_T = R_T\tau_r/\tau_c$, reveals that $p^{\text{opt}} \approx 0.23$, such that $\Delta^{\text{opt}} \approx 2\tau_c$. Interestingly, this is what Eq. (20) predicts: In an optimally designed system each receptor molecule should be sampled roughly twice every correlation time τ_c. Increasing X_T beyond that given by Eq. (30) means that the sampling interval becomes shorter than the receptor correlation time, creating redundant samples of the receptor state that do not provide any additional information on the average receptor occupancy from which the ligand concentration is inferred.

These observations indeed explain Figs. 3(a) and 3(b). To capitalize on the mechanism of time averaging, multiple independent concentration measurements per receptor must be taken, meaning $\tau_r > \tau_c$; in addition, to be able to store these measurements X_T must at least be $R_T\tau_r/\tau_c$. Consequently, when X_T is increased at fixed R_T, the sensing precision first rises with X_T because X_T limits the number of independent concentration measurements [Fig. 3(a)]; at the same time, to allow for an increase in the number of independent measurements with X_T, τ_r must also rise [Fig. 3(b)]. Yet, to maintain the dynamic gain $\tilde{g}_{L\to p_{\tau_r}}$ [Eq. (3)] and to contain the dynamical error [Eq. (26)], τ_r cannot rise indefinitely, which means that at some point the number of independent concentration measurement is no longer limited by X_T but rather by $R_T\tau_r/\tau_c$. The sensing precision now saturates and the system has entered the Berg-Purcell regime, where the optimal integration time arises from a trade-off between time averaging, the dynamic gain, and the dynamical error. Conversely, when R_T is increased at fixed X_T, the sensing precision first rises because it is initially limited by R_T. Yet the optimal integration time now decreases because *per receptor* less readout molecules become available and hence less receptor states can be stored: $X_T/R_T \approx \tau_r/\tau_c$ decreases.

Still, a number of questions remain: What is the optimal design in terms of protein copies and time, i.e., R_T, X_T, and τ_r? The resource allocation principle Eq. (30) predicts X_T for a given R_T and τ_r, but does not predict what τ_r should be. In fact, it merely constitutes one constraint on three variables, R_T, X_T, and τ_r (we assume that τ_c is set by the ligand concentration). To uniquely determine the optimal design that maximizes the sensing precision, we need to impose a second constraint, namely, on the costs of these cellular resources. Second, how accurate is the prediction of the allocation principle Eq. (30)? To what extent does the globally optimal system that is allowed to relax the constraint of the allocation principle still obey this principle?

B. Optimal design

To uniquely determine the optimal design, i.e., specify R_T, X_T, and τ_r, we need to impose a constraint that is determined by the cellular costs associated with these resources. What the relevant constraint is, and what the costs associated with these resources are, ultimately needs to be determined experimentally. Yet we can ask how sensitive the optimal design is to the precise nature of the constraint and the degree to which the allocation principle can predict it.

To address these questions, we here assume that the dominant cost of the sensing machinery is the production of the proteins, not the power to run it. We thus assume that the cost function is given,

$$C = R_T + c_X X_T, \tag{32}$$

where c_X sets the relative cost of making a readout versus a receptor protein. To determine the optimal design, we then maximize the sensing precision $I(x^*;L)$ for a given resource constraint C. The black dot in Fig. 3(a) shows the design $(R_T^{\text{opt}}, X_T^{\text{opt}})$ that maximizes the sensing precision along the gray line of a given resource constraint $C = R_T + X_T$, with $c_X = 1$; it is the point where a contour line of $I(x^*;L)$ runs parallel to the constraint C. The black line in Figs. 3(a) and 3(b) is then a parametric curve of the optimal design $(R_T^{\text{opt}}, X_T^{\text{opt}})$ for different values of C. The black lines in Fig. 4 show the same data: the sensing precision [Fig. 4(a)], the number of receptor (Fig. 4(b), solid line) and readout proteins [Fig. 4(b), dashed line], and the integration time [Fig. 4(c)] in the optimal system, as a function of the resource cost C.

As expected, the sensing precision increases with the total number of proteins C. Moreover, as predicted by the optimal allocation principle, R_T and X_T rise together in the optimal system [Fig. 3(a), Fig. 4(b)]. In fact, τ_r^{opt} remains constant as a function of C up to $C \sim R_T, X_T \approx 10^4$–$10^5$ before it drops to zero [Fig. 4(c)]. This can be understood by noting that until this crossover point, the sensing error is dominated by the sampling error. In this regime, the optimal integration time arises from a trade-off between the need to minimize the sampling error via time averaging and the competing demand to maximize the dynamic gain. This antagonistic interplay indeed gives rise to a constant optimal integration τ_r. However, at around $C \sim R_T, X_T \approx 10^4$–$10^5$, the increase in R_T and X_T has caused the sampling error to go down so much that it becomes comparable to the dynamical error, and from this point onwards both are reduced together by decreasing τ_r.

The resource cost C at which the dynamical error becomes dominant over the sampling error depends on $\sigma_L/\overline{L}$ and the receptor correlation time τ_c. As Eq. (26) shows, increasing the width of the signal distribution, $\sigma_L/\overline{L}$, increases the magnitude of the dynamical error, such that the crossover point shifts to lower C. Specifically, while, as Fig. 4 shows, for $\sigma_L/\overline{L} = 10^{-2}$ the crossover is at $C \sim 10^4$–10^5, for $\sigma_L/\overline{L} = 1$ the crossover point reduces to $C \sim 10^2$–10^3; see also Ref. [16], where a similar result was shown. Increasing the receptor correlation time τ_c makes time integration harder, which increases the optimal integration time, and raises the sampling error. Yet, as Eq. (26) reveals, increasing τ_c also increases the dynamical error, such that, perhaps surprisingly, the crossover point is hardly affected (with C changing less than twofold when τ_c is varied

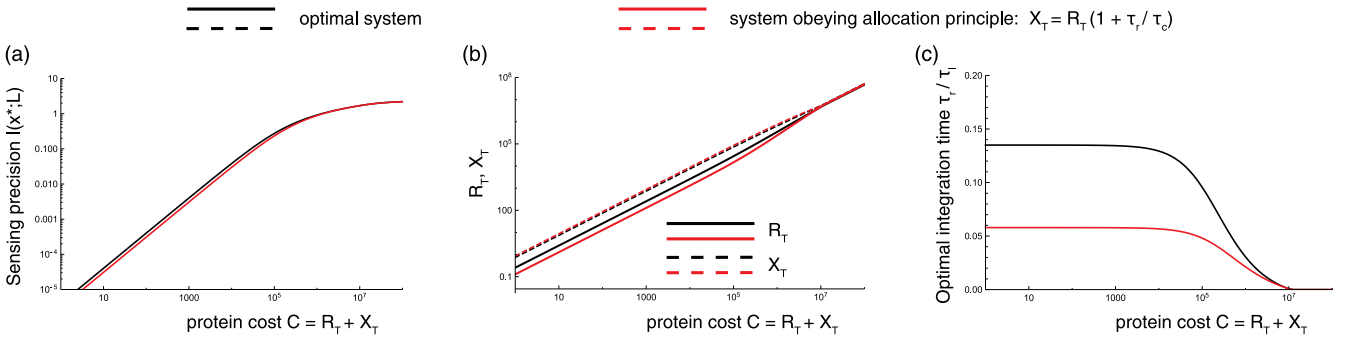

FIG. 4. The optimal resource allocation principle accurately describes the optimal system. The panels compare as a function of the protein cost $C = R_T + X_T$, the sensing precision $I(x^*;L)$, and design (R_T, X_T, τ_r) of the globally optimal system (black lines), where $I(x^*;L)$ has been optimized over R_T, X_T, τ_r, and p, to the precision and design of the optimal system that is constrained to obey the resource allocation principle $X_T = R_T(1 + \tau_r/\tau_c)$ (red lines); here $I(x^*;L)$ is also optimized over p and R_T, X_T, τ_r, but the allocation principle imposes a constraint that removes one degree of freedom between the latter three. See also Figs. 3(a) and 3(c). (a) The sensing precision $I(x^*;L)$ as a function of the protein cost $C = R_T + X_T$ for the globally optimal system (black line) and the optimal system that obeys the resource allocation principle (red line). (b) The number of receptors R_T (solid line) and the number of readout proteins X_T (dashed line) as a function of protein cost for for the globally optimal system (black lines) and the optimal system that obeys the resource allocation principle (red lines). (c) The integration time τ_r for the globally optimal system (black line) and the optimal system that obeys the resource allocation principle (red line). The receptor correlation time is $\tau_c/\tau_L = 10^{-2}$ and the relative width of the signal distribution is $\sigma_L/\bar{L} = 10^{-2}$.

tenfold). The concentrations of signaling proteins are typically in the micromolar range, such that the typical copy numbers scale with the size of the cell. For the chemotaxis system of *E. coli*, the copy numbers of the messenger protein CheY and the receptors and their associated kinase CheA are in the range 10^3–10^4, depending on the strain and the growth medium [21]. For eukaryotic signaling proteins, copy numbers are often in the range $10^4 - 10^5$, although some signaling proteins are also present at higher copy numbers of even 10^6 [22–24]. Clearly, while the precise crossover between the sampling-error-dominated regime and the dynamical-error-dominated one depends on the strength of the signal fluctuations $\sigma_L/\bar{L}$, which depends on the environment [16], our results show that the different regimes are likely to be biologically relevant.

C. Accuracy of optimal allocation principle

To assess the accuracy of the resource allocation principle, we compute the sensing precision $I(x^*;L)$ as a function of R_T and X_T for the optimal system that is forced to obey this principle: we thus optimize for each (R_T, X_T) the sensing precision over the receptor occupancy p while the integration time τ_r is set by the allocation principle $X_T = R_T(1 + \tau_r/\tau_c)$. Figure 3(c) shows the result. As before, we also compute for each resource constraint $C = R_T + c_X X_T$, with $c_X = 1$, the combination of R_T and X_T that maximizes the sensing precision, and plot this as a function of C (red line). It is seen that both the sensing precision and the optimal design (R_T, X_T) of the system that is constrained to obey the resource allocation principle are similar to those of the globally optimal system, shown in Fig. 3(a).

Figure 4 compares in more detail the characteristics of the system that obeys the allocation principle (red lines) to those of the globally optimal system (black lines). It is clear that the allocation principle predicts the optimal system remarkably well. This is because the number of receptors and their integration time, $R_T\tau_r/\tau_c$, and the number of readout proteins X_T limit sensing like weak links in a chain. The sensing precision is limited by the limiting resource, and in an optimally designed system, obeying Eq. (30), each resource is equally limiting. This simple principle explains why these resources cannot compensate each other, and why the contour lines of the sensing precision as a function of R_T and X_T in Fig. 3(a) and Fig. 3(c) have this distinct kneelike shape. The sensing precision can be raised only by increasing R_T and X_T together.

D. Dependence on resource costs

While the allocation principle gives a good description of the optimal system, a close inspection of Fig. 4 reveals that there are small but noticeable differences between the globally optimal system and the system that is forced to obey the allocation principle. In particular, while the contour lines have a kneelike shape, which stems from the fact that R_T and X_T limit sensing like links in a chain, the bend in the contour lines is still smooth. This is because the receptor occupancy p differs in the two limits of the sensing precision in Eqs. (28) and (29): while in the limit that the receptors are limiting the optimal receptor occupancy $p \to 1/2$, in the regime that the readouts are limiting $p \to 0$. Second, in the globally optimal system the optimal integration time $\tau_r^{\rm opt}$ is larger than that of the system that obeys the allocation principle [Fig. 4(c)]. This can be understood by noting that, for the parameter settings of Figs. 3 and 4, the sampling error dominates over the dynamical error (unless C becomes very large, in which case the differences between these systems disappear because time integration is no longer needed). This means that reducing the sampling error via time averaging is key. To make optimal use of the expensive readouts for time averaging, it is vital to ensure that they store receptor states and concentration measurements that are independent. This can be achieved by increasing the integration time, which makes it more likely that the sampling interval Δ is larger than the receptor correlation time τ_c. However, increasing the integration time too

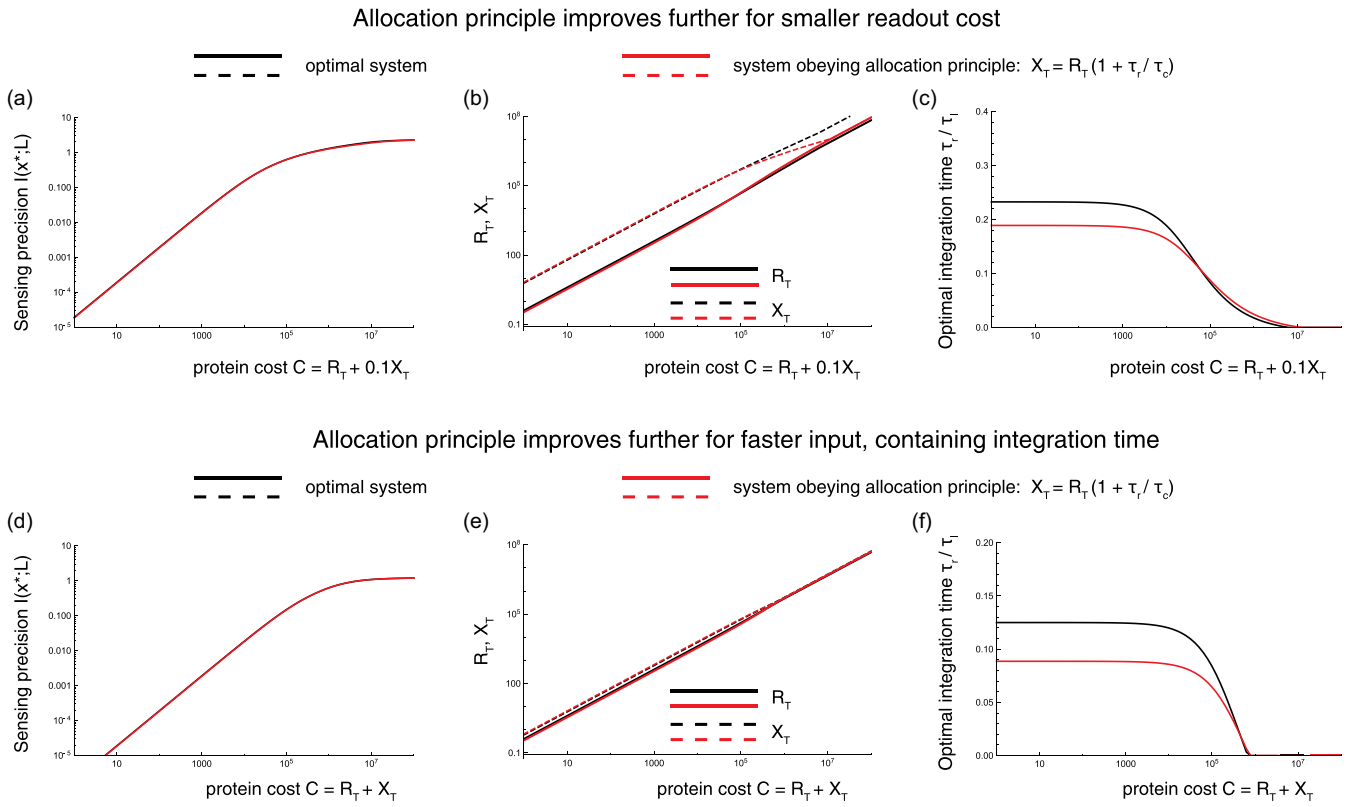

FIG. 5. The predictive power of the resource allocation principle improves further when the readout cost decreases or the input varies more rapidly, containing the integration time. The panels compare as a function of the protein cost $C = R_T + c_X X_T$ the sensing precision $I(x^*; L)$ and design (R_T, X_T, τ_r) of the globally optimal system (black lines), where $I(x^*; L)$ has been optimized over R_T, X_T, τ_r, and p, to the precision and design of the optimal system that is constrained to obey the resource allocation principle $X_T = R_T(1 + \tau_r/\tau_c)$ (red lines); here $I(x^*; L)$ is also optimized over p and R_T, X_T, τ_r, but the allocation principle imposes a constraint that removes one degree of freedom between the latter three. Top row (a–c) Relative cost of readout compared to receptor is decreased tenfold, $c_X = 0.1$. Bottom row (d, e) Input timescale τ_L is decreased tenfold compared to τ_c. (a, d) The sensing precision $I(x^*; L)$ as a function of the protein cost $C = R_T + X_T$ for the globally optimal system (black line) and the optimal system that obeys the resource allocation principle (red line). (b, e) The number of receptors R_T (solid line) and the number of readout proteins X_T (dashed line) as a function of protein cost for for the globally optimal system (black lines) and the optimal system that obeys the resource allocation principle (red lines). (c, f) The integration time τ_r for the globally optimal system (black line) and the optimal system that obeys the resource allocation principle (red line). The receptor correlation time is $\tau_c/\tau_L = 10^{-2}$, and the relative width of the signal distribution is $\sigma_L/\bar{L} = 10^{-2}$.

much will increase the sensing error because the dynamic gain becomes too low (and for large C also the dynamical error too large).

These observations suggest that the predictive power of the allocation principle improves further if the readout proteins become less costly so that the cost of redundant receptor sampling becomes milder, or if the pressure to contain the integration time becomes larger, for example when the input varies more rapidly. Figure 5 confirms these predictions. The top row shows the comparison between the optimal system and that constrained to obey the resource allocation principle when the readout cost is reduced tenfold, and the bottom row shows the comparison when the input timescale τ_L is decreased tenfold. Clearly, the predictive power of the optimal allocation principle has improved even further.

IV. DISCUSSION

In this paper, we have extended the sampling framework of Ref. [15] to time-varying signals. This framework views the signaling network as a device that discretely samples the receptor state. It reveals that the sensing error consists of two distinct contributions: the sampling error and the dynamical error. The benefit of viewing the network as a sampling device is that the results are intuitive. The important quantities in any sampling protocol are the number of samples, their spacing, their accuracy, and the dynamics of the signal to be sampled. The larger the number of samples, the lower the sampling error; the further apart they are, the more independent they are, which also lowers the sampling error; the higher their accuracy, the lower the sampling error [15]. Here we show then when the input signal fluctuates in time, the timescale on which the samples are taken also becomes important. More recent samples provide more reliable information on the current concentration which the cell aims to estimate than samples taken further back into the past. In particular, the lifetime of the samples, set by τ_r, should be shorter than the timescale τ_L on which the ligand concentration fluctuates. If not, a systematic error arises, the dynamical error, which cannot be eliminated by taking more samples.

While the sampling framework explicitly takes into account that the information from the ligand concentration is relayed to the readout via the receptor, the cell does ultimately infer the concentration from the readout. Our final result, Eq. (26), is indeed identical to that obtained by a straightforward linear-noise calculation of the mutual information $I(L;x^*)$ between the ligand concentration and the readout, as described in Appendix E. This can also be understood as follows: Because the average number of samples $\overline{N}$ is a constant, it follows from Eq. (5) that the variance in x^* given an input L is $\sigma^2_{x^*|L} = \sigma^2_{\hat{p}_{\tau_r}}\overline{N}^2$ while the gain from L to x^* is $\tilde{g}^2_{L\to x^*} = \tilde{g}^2_{L\to p_{\tau_r}}\overline{N}^2$. Consequently, the absolute error $(\delta\hat{L})^2$ in estimating the concentration via x^*, $(\delta\hat{L})^2 = \sigma^2_{x^*|L}/\tilde{g}^2_{L\to x^*}$, is the same as that of Eq. (1). In summary, because the instantaneous number of active readout molecules x^* reflects the average receptor occupancy p_{τ_r} over the past τ_r, estimating the ligand concentration from x^* is no different from inferring it from the average receptor occupancy $\hat{p}_{\tau_r} = x^*/\overline{N}$.

In Ref. [16] we derived the same principal result, Eq. (26), but via a different route, appealing to the linear-noise approximation. The added value of the current approach, based on the sampling framework of Ref. [15], is twofold. First, the fact that the principal result can be rigorously derived via the sampling framework demonstrates unambiguously that cells implement the mathematical operation of time integration via molecules that execute a stochastic and discrete sampling protocol. Second, this framework naturally reveals the origins of the distinct contributions to the sensing error: the sampling error and the dynamical error; Fig. 2 sums up the origins of these contributions. The framework elucidates these sources not only intuitively, but derives them also rigorously. For example, it shows how the dynamical error emerges from the variance in the estimate of the receptor occupancy that arises from the fact that a given current ligand concentration, which the cell aims to estimate, corresponds to an ensemble of past ligand trajectories, from which the cell actually infers the current concentration [see Fig. 1(d)]. Understanding these contributions not only provides insight into the origins of the sensing error, but also naturally gives rise to the optimal resource allocation principle.

The optimal resource allocation principle states that in an optimally designed system the number of independent concentration measurements at the receptor level, $R_T\tau_r/\tau_c$, equals the number of readout proteins that are necessary and sufficient store these measurements, X_T [15]. However, this principle as such does not specify the integration time τ_r. There does exist an optimal integration time that maximizes the sensing precision, which arises from a trade-off between time averaging, the dynamic gain, and the dynamical error [16]. Yet its value, as well as R_T and X_T in the optimal system, depends on the dynamics of the input signal and the (relative) costs of making the receptor and readout proteins.

We have therefore applied our theory to study the optimal design that maximizes the sensing precision given a constraint on the total protein cost and the degree to which this optimal design obeys the resource allocation principle. The optimal design as such does depend on the relative cost of producing readout versus receptor proteins: cheaper readout proteins make time averaging more beneficial, which raises the optimal integration time and the ratio of the number of readout over receptor proteins, precisely as predicted by our allocation principle [compare Figs. 5(b) and 5(c) with Figs. 4(b) and 4(c)]. However, these figures also show that all the optimal systems obey, to a good approximation, the optimal resource allocation principle. This principle is thus robust to the relative costs of the cellular resources. This is because these resources are fundamental and cannot significantly compensate each other. In an optimally designed system, each of these resources is equally limiting so that none resource is in excess. Resources that are in excess cannot significantly reduce the sensing error, no matter how cheap they are.

Signaling systems do not always aim to estimate the current ligand concentration, as we have assumed here. A prime example is the chemotaxis system of the bacterium *E. coli*, which aims to estimate whether the concentration has changed, by taking a temporal derivative of the input signal. This derivative is taken by two antagonistic systems, which operate on two distinct timescales. Ligand binding rapidly changes the activity of the receptor, which, via a push-pull network as studied here, then leads to a fast change in the phosphorylation state of the downstream messenger protein CheY. This effect is, however, counteracted on longer timescales via slow (de)methylation of the receptor. These reactions together allow the system to take a temporal derivative, essentially subtracting the past ligand concentration from the current concentration. The accuracy of the estimate of the current concentration, the topic of our study, provides a lower bound on the precision of the estimate of this temporal derivative [16]. For future work it would be of interest to extend our analysis and study how resources constrain the performance of signaling systems that need to take a temporal derivative of the input signal.

ACKNOWLEDGMENTS

This work is part of the Dutch Research Council (NWO) and was performed at the research institute AMOLF. We would like to thank Age Tjalma for a critical reading of our manuscript.

APPENDIX A: ERROR FROM STOCHASTICITY IN NUMBER OF SAMPLES: Eq. (10)

The first term of Eq. (8) describes the noise that arises from the stochasticity in the number of samples N. It can be written as

$$\mathrm{var}[E(\hat{p}_{\tau_r}|N)] = \mathrm{var}\left[\frac{1}{\overline{N}}E\left(\sum_{i=1}^{N} n(t_i)\middle| N\right)\right], \tag{A1}$$

where we have dropped the subscript i on n_i [compare against Eq. (6)] because in estimating the average receptor occupancy we can focus on a single receptor. The above average can be written as

$$E\left(\sum_{i=1}^{N} n(t_i)\middle| N\right) = N\overline{E\langle n(t_i)\rangle}_{\delta L(t)} \tag{A2}$$

$$= N\left(p + \overline{E\langle \delta n(t_i)\rangle}_{\delta L(t)}\right) \tag{A3}$$

$$= N(p + \overline{\tilde{g}\delta L(t)}) \tag{A4}$$

$$= Np. \tag{A5}$$

Here the angular brackets $\langle \dots \rangle_{\delta L(t)}$ denote an average over the ligand binding state of the receptor, with the subscript $\delta L(t)$ indicating that the average is to be taken for a given $\delta L(t)$. The expectation E denotes an average over all samples times t_i, and the overline indicates an average over $\delta L(t)$. In going from the second to the third line we have used that $\delta p_{\tau_r} = \tilde{g}\delta L(t)$ [16], with $\tilde{g}$ the short-hand notation for $\tilde{g} = \tilde{g}_{L\to p_{\tau_r}}$, as also used below unless stated otherwise. Hence, Eq. (A1) becomes

$$\mathrm{var}\big[E\left(\hat{p}_{\tau_r}|N\right)\big] = \mathrm{var}\left[\frac{N}{\overline{N}}p\right] \tag{A6}$$

$$= \frac{p^2}{\overline{N}^2}\mathrm{var}[N] \tag{A7}$$

$$= \frac{p^2}{\overline{N}}. \tag{A8}$$

APPENDIX B: VARIANCE IN AVERAGE RECEPTOR OCCUPANCY FOR FIXED NUMBER OF SAMPLES: Eq. (12)

Equation (12) gives the variance in the average receptor occupancy for a fixed number of samples. To derive it, we note that

$$\mathrm{var}\left(\frac{\sum_{i=1}^N n_i(t_i)}{N}\middle| N\right)_{\delta L(t)} \tag{B1}$$

$$= \frac{\overline{E\left\langle\left(\sum_{i=1}^N n_i(t_i)\right)^2\right\rangle_{\delta L(t)}} - \overline{E\left\langle\sum_{i=1}^N n_i(t_i)\right\rangle^2_{\delta L(t)}}}{N^2} \tag{B2}$$

$$= \frac{\overline{E\left\langle\left(\sum_{i=1}^N n_i(t_i)\right)^2\right\rangle_{\delta L(t)}} - N^2\overline{[p+\tilde{g}\delta L(t)]^2}}{N^2} \tag{B3}$$

$$= \frac{N\overline{[p+\tilde{g}\delta L(t)]} + N(N-1)\overline{E\langle n_i(t_i)n_j(t_j)\rangle_{\delta L(t)}}}{N^2} - \overline{[p+\tilde{g}\delta L(t)]^2} \tag{B4}$$

$$= \frac{N\overline{[p+\tilde{g}\delta L(t)]} - N\overline{[p+\tilde{g}\delta L(t)]^2}}{N^2} + \frac{N(N-1)\overline{E\langle\tilde{\delta}n_i(t_i)\tilde{\delta}n_j(t_j)\rangle_{\delta L(t)}}}{N^2} \tag{B5}$$

$$= \frac{p(1-p) - \tilde{g}^2\sigma_L^2}{N} + \frac{N(N-1)\overline{E\langle\tilde{\delta}n_i(t_i)\tilde{\delta}n_j(t_j)\rangle_{\delta L(t)}}}{N^2}. \tag{B6}$$

Here $\tilde{\delta}n_i(t_i) \equiv n_i(t_i) - \langle n_i(t_i)\rangle_{\delta L(t)} = n_i(t_i) - [p + \langle\delta n_i(t_i)\rangle_{\delta L(t)}]$ is the deviation away from the average receptor occupancy $\langle n_i(t_i)\rangle = p + \langle\delta n_i(t_i)\rangle_{\delta L(t)}$ at time t_i when the ligand concentration at time t is $\delta L(t)$. In Eq. (B6), E denotes, as before, an average over the sampling times of the receptor. The average of $n_i(t_i)$ over the sampling times t_i given $\delta L(t)$, is $E[\langle n_i(t_i)\rangle_{\delta L(t)}] = p + E\langle\delta n_i(t_i)\rangle_{\delta L(t)} = p + \tilde{g}\delta L(t)$ (noting that $\delta p_{\tau_r} = \tilde{g}\delta L(t)$ [16]). In addition, $\sigma_L^2 = \langle\delta L(t)^2\rangle$ is the variance of the ligand concentration, and in going from Eqs. (B3) to (B4) we have exploited that $n^2 = n$. The quantity $\overline{E\langle\tilde{\delta}n_i(t_i)\tilde{\delta}n_j(t_j)\rangle_{\delta L(t)}}$ is the covariance of the receptor occupancy given that the ligand concentration at time t is $\delta L(t)$, and then averaged over all values of $\delta L(t)$, as indicated by the overline. This quantity has a contribution from the receptor switching noise and the dynamical error resulting from the ligand fluctuations.

While $\overline{E\langle\tilde{\delta}n_i(t_i)\tilde{\delta}n_j(t_j)\rangle_{\delta L(t)}} = \overline{E\langle n_i(t_i)n_j(t_j)\rangle_{\delta L(t)}} - \overline{E\langle n_i(t_i)\rangle_{\delta L(t)}\langle n_j(t_j)\rangle_{\delta L(t)}}$ is the quantity that we need to compute, it is difficult to compute straightforwardly. We can, however, exploit the following trick [20]. Denoting $x = n_i(t_i)$, $y = n_j(t_j)$ and $z = \delta L(t)$, we can write the quantity of interest as $\overline{E\langle\tilde{\delta}n_i(t_i)\tilde{\delta}n_j(t_j)\rangle_{\delta L(t)}} = \overline{E\langle xy\rangle_z} - \overline{E\langle x\rangle_z E\langle y\rangle_z}$. We can then exploit the following relation:

$$\overline{E\langle\delta x\delta y\rangle_z} = \overline{E\langle xy\rangle_z} - \overline{E\langle x\rangle_z E\langle y\rangle_z} + \overline{E\langle x\rangle_z E\langle y\rangle_z} - \overline{E\langle x\rangle_z}\;\overline{E\langle y\rangle_z} \tag{B7}$$

$$= \overline{E\langle xy\rangle_z} - \overline{E\langle x\rangle_z E\langle y\rangle_z} + \tilde{g}^2\sigma_L^2. \tag{B8}$$

Importantly, $\overline{E\langle\delta x\delta y\rangle_z}$ is the covariance related to the deviation of the receptor occupancy from the mean p, which is easier to compute that the deviation from $p + \tilde{g}\delta L(t)$. Inserting the above result into Eq. (B6) yields

$$\mathrm{var}\left(\frac{\sum_{i=1}^N n_i(t_i)}{N}\right)_{\delta L(t)} = \frac{p(1-p)}{N} + \overline{E\langle\delta n_i(t_i)\delta n_j(t_j)\rangle}_{\delta L(t)} - \tilde{g}^2\sigma_L^2, \tag{B9}$$

where we have used that $N(N-1) \approx N^2$ for $N \gg 1$.

APPENDIX C: RECEPTOR SWITCHING NOISE: Eq. (17)

To average Eq. (16) over the sampling times, it is convenient to express and evaluate the integrals in terms of $\lambda = 1/\tau_{\mathrm{L}}$, $\mu = 1/\tau_{\mathrm{c}}$, and $\mu' = 1/\tau_{\mathrm{r}}$. Using that the probability that a readout molecule at time t has taken a sample of the receptor at an earlier time t_i is $p(t_i|\mathrm{sample}) = e^{-(t-t_i)/\tau_{\mathrm{r}}}/\tau_{\mathrm{r}}$ [15], we obtain

$$E[\mathrm{covR}(n_i(t_i), n_j(t_j))] = \frac{p(1-p)\mu'^2}{R_{\mathrm{T}}}\int_{-\infty}^{t} dt_i \int_{-\infty}^{t} dt_j e^{-\mu'(t-t_i)}e^{-\mu'(t-t_j)}e^{-\lambda|t_j-t_i|} \tag{C1}$$

$$= \frac{p(1-p)\mu'^2}{R_{\mathrm{T}}}e^{-2\mu' t}\int_{-\infty}^{t} dt_j e^{2\mu' t_j} 2\int_0^{\infty} d\tilde{\Delta}e^{-(\mu'+\mu)\tilde{\Delta}} \tag{C2}$$

$$= \frac{p(1-p)}{R_{\mathrm{T}}}\frac{\tau_{\mathrm{c}}}{\tau_{\mathrm{c}}+\tau_{\mathrm{r}}} \simeq \frac{p(1-p)}{R_{\mathrm{T}}}\frac{\tau_{\mathrm{c}}}{\tau_{\mathrm{r}}}, \tag{C3}$$

where $\tilde{\Delta} = |t_j - t_i|$ and in the last line we have used that typically $\tau_{\mathrm{r}} \gg \tau_{\mathrm{c}}$. The factor $1/R_{\mathrm{T}}$ arises from the Krokecker delta δ_{ij} in Eq. (16), taking into account that the receptors bind the ligand independently.

APPENDIX D: RECEPTOR VARIANCE FROM SIGNAL VARIATIONS: Eq. (23)

To obtain the variance in the receptor occupancy that arises from the signal fluctuations $\delta L(t0$, $\overline{E[\mathrm{covS}(n_i(t_i), n_j(t_j))]}$ in

Eq. (15), we recognize that the averaging over $\delta L(t)$ can be performed before the averaging over the sampling times, such that $\overline{E[\mathrm{covS}(n_i(t_i), n_j(t_j))]} = E[\overline{\mathrm{covS}(n_i(t_i), n_j(t_j))}]$ with

$$\overline{\mathrm{covS}(n_i(t_i), n_j(t_j))} = \rho_n^2 \int_{-\infty}^{t_i} dt' \int_{-\infty}^{t_j} dt'' e^{-(t_i-t')/\tau_c} \overline{\langle \delta L(t')\delta L(t'')\rangle}_{\delta L(t)} \times e^{-(t_j-t'')/\tau_c}. \tag{D1}$$

We can now exploit that the correlation function of the input signal is given by $\overline{\langle \delta L(t')\delta L(t'')\rangle}_{\delta L(t)} = \langle \delta L(t')\delta L(t'')\rangle = \sigma_L^2 e^{-\lambda|t''-t'|}$, with $\lambda = 1/\tau_L$. Inserting this into Eq. (D1) and integrating it yields

$$\overline{\mathrm{covS}(n_i(t_i), n_j(t_j))} = \rho_n^2 \sigma_L^2 \frac{\lambda e^{-\mu(t_j-t_i)} - \mu e^{-\lambda(t_j-t_i)}}{\mu(\lambda^2-\mu^2)}, \tag{D2}$$

with $\mu = 1/\tau_c$ defined as before. Defining $\mu' = 1/\tau_r$, we now again average over the sample times

$$E[\overline{\mathrm{covS}(n_i(t_i), n_j(t_j))}] \tag{D3}$$

$$\mu'^2 \int_{-\infty}^{t} dt_i \int_{-\infty}^{t} dt_j e^{-\mu'(t-t_i)} \overline{\mathrm{covS}(n_i(t_i), n_j(t_j))} e^{-\mu'(t-t_j)} \tag{D4}$$

$$= \rho_n^2 \sigma_L^2 \frac{\mu'(\lambda+\mu+\mu')}{\mu(\mu+\lambda)(\mu+\mu')(\mu'+\lambda)} \tag{D5}$$

$$= \frac{\rho_n^2 \mu'^2 \sigma_L^2}{(\mu+\lambda)^2(\mu'+\lambda)^2} \frac{(\lambda+\mu+\mu')(\mu+\lambda)(\mu'+\lambda)}{\mu'\mu(\mu+\mu')} \tag{D6}$$

$$= \tilde{g}^2 \sigma_L^2 \frac{(\lambda+\mu+\mu')(\mu+\lambda)(\mu'+\lambda)}{\mu'\mu(\mu+\mu')} \tag{D7}$$

$$= \tilde{g}^2 \sigma_L^2 \left(1+\frac{\tau_c}{\tau_L}\right)\left(1+\frac{\tau_r}{\tau_L}\right)\left(1+\frac{\tau_c\tau_r}{\tau_L(\tau_c+\tau_r)}\right). \tag{D8}$$

APPENDIX E: SENSING PRECISION BASED ON OUTPUT x^* DERIVED VIA THE LINEAR-NOISE APPROXIMATION

An alternative approach to derive the sensing error,, which, we argue, is less informative, is to focus directly on the output x^*, and not explicitly address the fact that the information on the input concentration is relayed to the output via the receptor. In this view, the cell thus infer the current ligand concentration $L(t)$ directly from the instantaneous concentration of the output $x^*(t)$ and by inverting the input-output relation $\overline{x^*}(L)$. Since the ligand concentration fluctuates in time, and because the system will, in general, not respond instantly to these fluctuations, the input-output relation that the system must employ is the *dynamic* input-output relation $\overline{x^*}(L)$, which yields the average readout concentration $\overline{x^*}$ *given that* the current value of the time-varying signal is $L(t)$; here the average is not only over the noise sources in the propagation of the signal from the input L to the output x^*—the receptor-ligand binding noise and the readout-phosphorylation noise [see Fig. 1(c)]—but also over the ensemble of input trajectories that each have the same current concentration $L(t)$ [see Fig. 1(d)] [18–20].

Sensing error. Linearizing $\overline{x^*}(L)$ around the mean concentration $\overline{L}$ and using the rules of error propagation, the expected error in the concentration estimate is then

$$(\delta\hat{L})^2 = \frac{\sigma^2_{x^*|L}}{\tilde{g}^2_{L\to x^*}}. \tag{E1}$$

In this expression, $\sigma^2_{x^*|L}$ quantifies the width of the distribution of the output x^* *given* a value of the input signal L, while $\tilde{g}_{L\to x^*}$ is the dynamic gain, i.e., the slope of $\overline{x^*}(L)$ at $\overline{L}$.

Gaussian statistics. We can obtain the variance $\sigma^2_{x^*|L}$ and the dynamic gain $\tilde{g}_{L\to x^*}$ within the Gaussian framework of the linear-noise approximation [18]. The deviations of L and x^* away from their mean values are, respectively:

$$\delta L(t) = L(t) - \overline{L}, \tag{E2}$$

$$\delta x^*(t) = x^*(t) - \overline{x^*}. \tag{E3}$$

Since the dynamics of both L and x^* are stationary processes, we can choose to omit the explicit dependence on time, and simply write $\delta L(t) = \delta L$ and similarly for x^*. Defining the vector $\mathbf{v}$ with components $\delta L(t)$, $\delta x^*(t)$, the joint distribution can be written as

$$p(\mathbf{v}) = \frac{1}{\sqrt{2\pi^{2N}|\mathbf{Z}|}} \exp\left(-\frac{1}{2}\mathbf{v}^{\mathrm{T}}\mathbf{Z}^{-1}\mathbf{v}\right), \tag{E4}$$

where $\mathbf{Z}^{-1}$ is the inverse of the matrix $\mathbf{Z}$, which has the following form:

$$\mathbf{Z} = \begin{pmatrix} \sigma_L^2 & \sigma^2_{L,x^*} \\ \sigma^2_{L,x^*} & \sigma^2_{x^*} \end{pmatrix}. \tag{E5}$$

From Eq. (E4) it follows that the conditional distribution of δx^* given δL is

$$p(\delta x^*|\delta L) = \frac{1}{\left(2\pi\sigma^2_{x^*|L}\right)^{1/2}} \exp\left\{-\frac{[\delta x^* - \overline{\delta x^*}(\delta L)]^2}{2\sigma^2_{x^*|L}}\right\}. \tag{E6}$$

Dynamic gain. In Eq. (E6), $\overline{\delta x^*}(\delta L)$ is the average of the deviation $\delta x^*(\delta L) = x^*(\delta L) - \overline{x^*}$ of x^* from its mean $\overline{x^*}$ given that the input is $\delta L = \delta L(t)$; it describes the dynamic input relation $\overline{x^*}(L)$ around $L = \overline{L}$. It is given by $\overline{\delta x^*}(\delta L) = \sigma^2_{L,x^*}/\sigma_L^2 \delta L \equiv \tilde{g}_{L\to p_{\tau_r}} \delta L$, which defines the dynamic gain:

$$\tilde{g}_{L\to p_{\tau_r}} = \sigma^2_{L,x^*}/\sigma_L^2. \tag{E7}$$

Here σ_L^2 is the variance of the input and σ^2_{L,x^*} is the covariance between L and x^*, which is derived below.

Conditional variance. In Eq. (E6), the variance $\sigma^2_{x^*|L}$ is the variance in x^* given that the signal is L. It is given by $\sigma^2_{x^*|L} = |\mathbf{Z}|/\sigma_L^2$ [18], such that

$$\sigma^2_{x^*|L} = \sigma^2_{x^*} - \tilde{g}^2_{L\to p_{\tau_r}} \sigma_L^2, \tag{E8}$$

where $\sigma^2_{x^*}$ is the full variance of x^*. Indeed, in this Gaussian model, the total variance $\sigma^2_{x^*}$ in the output x^* can be decomposed into a contribution from the variance $\tilde{g}^2_{L\to x^*}\sigma_L^2$ due to variations in the signal itself, and a contribution from the variance $\sigma^2_{x^*|L}$ for a given value of the input L. The conditional variance $\sigma^2_{x^*|L}$ is shaped both by the noise in the propagation of the input L to the output x^*—stochastic receptor-ligand

binding and noisy readout activation—and by the dynamics of the input signal.

LNA description. To compute the (co)variances, we can employ the linear-noise approximation. The deviations of RL and x^* away from their steady-state values are given by:

$$\delta\dot{RL}(t) = \rho\delta L(t) - \mu\delta RL(t) + \eta_{RL}, \tag{E9}$$

$$\delta\dot{x^*}(t) = \rho'\delta RL(t) - \mu'\delta x^*(t) + \eta_{x^*}. \tag{E10}$$

In the first equation, $\mu = k_1\overline{L} + k_2 = {\tau_c}^{-1}$ is the inverse of the receptor correlation time τ_c, $\rho = R_T k_1(1-p) = p(1-p)R_T\mu/\overline{L}$, where $p = \overline{RL}/R_T = k_1\overline{L}/(k_2 + k_1\overline{L}) = k_1\overline{L}/\mu$ is the fraction of ligand-bound receptors.. In the second equation, $\rho' = k_f X_T(1-f) - k_{-f}X_T f$ and $\mu' = (k_f + k_{-f})pR_T + k_r + k_{-r} = {\tau_r}^{-1}$ is the inverse of the integration time τ_r, where $f = \overline{x}^*/X_T = (k_f pR_T + k_{-r})/[k_f + k_{-f})pR_T + k_r + k_{-r}] = (k_f pR_T + k_{-r})\tau_r$ is the fraction of phosphorylated readout molecules.

The noise functions are given by [25]

$$\langle \eta_{RL}^2 \rangle = 2\mu R_T p(1-p), \tag{E11}$$

$$\langle \eta_{x^*}^2 \rangle = 2\mu' X_T f(1-f), \tag{E12}$$

where the cross-correlations $\langle \eta_L \eta_{RL}\rangle = \langle \eta_{x^*}\eta_L\rangle = \langle \eta_{x^*}\eta_{RL}\rangle = 0$ are zero because receptor-ligand binding does not affect the total ligand concentration and the complex RL acts as a catalyst in the push-pull network [26].

We can then obtain the variances from the power spectra, $\sigma^2_{\alpha,\beta} = 1/(2\pi)\int_{-\infty}^{\infty} S_{\alpha\beta}(\omega)$, which can be obtained by solving Eqs. (E9)–(E12) in the Fourier domain:

$$\sigma^2_{x^*} = f(1-f)X_T + \frac{\rho'^2}{\mu'(\mu+\mu')}\left[p(1-p)R_T + \frac{\rho^2\sigma_L^2(\lambda+\mu+\mu')}{\mu(\lambda+\mu)(\lambda+\mu')}\right], \tag{E13}$$

$$\sigma^2_{RL} = p(1-p)R_T + \frac{\rho^2\sigma_L^2}{\mu(\mu+\lambda)}, \tag{E14}$$

$$\sigma^2_{L,RL} = \frac{\rho\sigma_L^2}{(\mu+\lambda)}, \tag{E15}$$

$$\sigma^2_{L,x^*} = \frac{\rho\rho'\sigma_L^2}{(\lambda+\mu)(\lambda+\mu')}, \tag{E16}$$

$$\sigma^2_{RL,x^*} = \frac{\rho'}{\mu'+\mu}\left[p(1-p)R_T + \frac{\rho^2\sigma_L^2(\mu'+\lambda+\mu)}{\mu(\lambda+\mu)(\lambda+\mu')}\right]. \tag{E17}$$

Signal-to-noise ratio (SNR). Combining the expression for the definition of SNR, given in Eq. (2), with Eq. (E1) then yields the sensing error, the inverse SNR:

$$\mathrm{SNR}^{-1} = \frac{\sigma^2_{x^*|L}}{\tilde{g}^2_{L\to x^*}\sigma_L^2} = \frac{\sigma_L^2\sigma^2_{x^*}}{\sigma^4_{L,x^*}} - 1, \tag{E18}$$

where we have used Eqs. (E7) and (E8). Using the expressions for the variance for x^*, Eq. (E13), and the covariance between L and x^*, Eq. (E17), the signal-to-noise ratio reads

$$\begin{aligned}\mathrm{SNR}^{-1} = {} & \frac{(\lambda+\mu)^2(\lambda+\mu')^2}{\rho^2\rho'^2\sigma_L^2} f(1-f)X_T \\ & + \frac{(\lambda+\mu)^2(\lambda+\mu')^2}{\sigma_L^2\mu'(\mu+\mu')\rho^2} p(1-p)R_T \\ & + \frac{(\lambda+\mu)(\lambda+\mu')(\lambda+\mu+\mu')}{\mu\mu'(\mu+\mu')} - 1.\end{aligned} \tag{E19}$$

This expression is identical to the central result of our paper, Eq. (26), but more difficult to interpret intuitively and impedes an analysis of the fundamental resources required for sensing. Yet this analysis does make clear that this SNR also yields the mutual information $I(L;x^*) = 1/2\ln(1+\mathrm{SNR})$ between L and x^* [18].

[1] J. Boeckh, K.-E. Kaissling, and D. Schneider, Insect olfactory receptors, Cold Spring Harbor Symp. Quant. Biol **30**, 263 (1965).

[2] H. C. Berg and E. M. Purcell, Physics of chemoreception, Biophys. J. **20**, 193 (1977).

[3] V. Sourjik and H. C. Berg, Binding of the *Escherichia coli* response regulator CheY to its target measured *in vivo* by fluorescence resonance energy transfer, Proc. Natl. Acad. Sci. USA **99**, 12669 (2002).

[4] M. Ueda and T. Shibata, Stochastic signal processing and transduction in chemotactic response of eukaryotic cells, Biophys J **93**, 11 (2007).

[5] P. R. ten Wolde, N. B. Becker, T. E. Ouldridge, and A. Mugler, Fundamental limits to cellular sensing, J. Stat. Phys. **162**, 1395 (2016).

[6] W. Bialek and S. Setayeshgar, Physical limits to biochemical signaling, Proc. Natl. Acad. Sci. USA **102**, 10040 (2005).

[7] K. Kaizu, W. De Ronde, J. Paijmans, K. Takahashi, F. Tostevin, and P. R. T. Wolde, The Berg-Purcell limit revisited, Biophys. J. **106**, 976 (2014).

[8] A. Mugler, A. Levchenko, and I. Nemenman, Limits to the precision of gradient sensing with spatial communication and temporal integration, Proc. Natl. Acad. Sci. USA **113**, E689 (2016).

[9] R. G. Endres and N. S. Wingreen, Maximum Likelihood and the Single Receptor, Phys. Rev. Lett. **103**, 158101 (2009).

[10] T. Mora and N. S. Wingreen, Limits of Sensing Temporal Concentration Changes by Single Cells, Phys. Rev. Lett. **104**, 248101 (2010).

[11] A. H. Lang, C. K. Fisher, T. Mora, and P. Mehta, Thermodynamics of Statistical Inference by Cells, Phys. Rev. Lett. **113**, 148103 (2014).

[12] D. Hartich and U. Seifert, Optimal inference strategies and their implications for the linear noise approximation, Phys. Rev. E **94**, 042416 (2016).

[13] T. Mora and I. Nemenman, Physical Limit to Concentration Sensing in a Changing Environment, Phys. Rev. Lett. **123**, 198101 (2019).

[14] A. Goldbeter and D. E. Koshland, An amplified sensitivity arising from covalent modification in biological systems, Proc. Natl. Acad. Sci. USA **78**, 6840 (1981).

[15] C. C. Govern and P. R. ten Wolde, Optimal resource allocation in cellular sensing systems, Proc. Natl. Acad. Sci. USA **111**, 17486 (2014).

[16] G. Malaguti and P. R. ten Wolde, Theory for the optimal detection of time-varying signals in cellular sensing systems, eLife **10**, e62574 (2021).

[17] T. E. Ouldridge, C. C. Govern, and P. R. ten Wolde, Thermodynamics of Computational Copying in Biochemical Systems, Phys. Rev. X **7**, 021004 (2017).

[18] F. Tostevin and P. R. ten Wolde, Mutual information in time-varying biochemical systems, Phys. Rev. E **81**, 061917 (2010).

[19] A. Hilfinger and J. Paulsson, Separating intrinsic from extrinsic fluctuations in dynamic biological systems, Proc. Natl. Acad. Sci. USA **108**, 12167 (2011).

[20] C. G. Bowsher, M. Voliotis, and P. S. Swain, The fidelity of dynamic signaling by noisy biomolecular networks, PLoS Comput. Biol. **9**, e1002965 (2013).

[21] M. Li and G. L. Hazelbauer, Cellular stoichiometry of the components of the chemotaxis signaling complex, J. Bact. **186**, 3687 (2004).

[22] S. Ghaemmaghami, W.-K. Huh, K. Bower, R. W. Howson, A. Belle, N. Dephoure, E. K. O'Shea, and J. S. Weissman, Global analysis of protein expression in yeast, Nature (London) **425**, 737 (2003).

[23] B. Schwanhäusser, D. Busse, N. Li, G. Dittmar, J. Schuchhardt, J. Wolf, W. Chen, and M. Selbach, Global quantification of mammalian gene expression control, Nature (London) **473**, 337 (2011).

[24] M. Zeiler, W. L. Straube, E. Lundberg, M. Uhlen, and M. Mann, A protein epitope signature tag (PrEST) library allows SILAC-based absolute quantification and multiplexed determination of protein copy numbers in cell lines, Mol. Cell. Proteomics **11**, O111.009613 (2012).

[25] P. B. Warren, S. Tânase-Nicola, and P. R. ten Wolde, Exact results for noise power spectra in linear biochemical reaction networks, J. Chem. Phys. **125**, 144904 (2006).

[26] S. Tanase-Nicola, P. B. Warren, and P. R. ten Wolde, Signal Detection, Modularity, and the Correlation between Extrinsic and Intrinsic Noise in Biochemical Networks, Phys. Rev. Lett. **97**, 068102 (2006).